Scalable PIC Packaging and Polarization Control in CPO

Florian Merget[a,b], Manuel Ackermann[a], Bin Shen[b], Rebecca Rodrigo[a], Huiyi Wang[a], Michael Wolz[c], Jeremy Witzens[*a,b]

[a]Institute of Integrated Photonics, Campus Boulevard 73, 52074 Aachen, Germany;
[b]aiXscale Photonics GmbH, Campus Boulevard 79, 52074 Aachen, Germany;
[c]GD Optical Competence GmbH, Zur Dornheck 24, 35764 Sinn, Germany

ABSTRACT

The emergence of co-packaged optics and of parallel optics pluggable form factors with an increased number of fibers poses new challenges for optical packaging technologies. We describe micro-optical interposers manufactured with isothermal glass molding that enable the parallelized connection of large fiber arrays with photonic integrated circuits in a low-rise form factor as well as the management of scrambled light polarization from a remote laser source coupled by single mode fiber. A resonantly assisted but temperature tolerant silicon photonics Mach-Zehnder modulator operated in lumped element configuration is co-developed for that purpose and a concept for a 6.4 Tb/s bi-directional light engine described.

Keywords: Co-packaged optics, isothermal glass molding, glass interposers, silicon photonics, resonantly assisted modulators, photonic packaging, electro-optic modulation

1. INTRODUCTION

Co-packaged optics (CPO) refers to the integration of electronic systems, such as a top-of-the-rack switch chip, with electro-optic transceivers in a single semiconductor package [1]. This removes printed circuit boards and their transmission lines, that are interposed between the switch chip and the electronics, and thus the signal distortion and attenuation they create. Simplification of the electronics made possible by this, in particular in systems linearly driving the electro-optic transceivers, have been estimated to enable a reduction of power consumption in the range of 25% to 50% from that associated to operating pluggable modules [2].

Electronic in-package chiplet integration technology has been leveraged to combine electronics with photonics [3]. However, a typical high-performance switch uses 64 modules with 2 to 8 fibers each, so that up to several hundred fibers have to be attached in a very small package, resulting in big challenges in photonic packaging. To be scalable to large port counts while maintaining alignment and mechanical integrity under thermal cycles, micro-optics interposed between the fibers and the photonic integrated circuit (PIC) should be made out of a material with a coefficient of thermal expansion (CTE) close to that of the chip, which can be achieved for example with certain types of silica glasses [4].

In addition, a growing school of thought argues that the lasers are better left out of the main CPO assembly and coupled to it via a fiber [1], [3]. This does not prevent the electro-optic modulators to be integrated inside the package and the electrical connections to be kept short. It also allows lasers to be operated at a lower temperature and thus at a higher wall-plug efficiency and facilitates their replacement if they fail. Since semiconductor lasers are one of the major failure sources in electro-optic modules, this appears a desirable path forward if interface losses are kept sufficiently low and polarization scrambling can be suppressed or managed. The latter can be solved by utilizing polarization maintaining fiber, although its precise angular alignment with the polarization of the laser and the interfaces of PICs can be a cost factor. On-chip recombination of the two light polarizations received from a regular single mode fiber can also be an option [5], although endless operation, while possible, requires a larger number of stages and is thus more complex [6].

Here, we present micro-optical interposers that have been scaled up to arrays of 32 optical ports on a 250 μm pitch, as well as progress towards advanced configurations incorporating polarization control (Section 2). In particular, one interposer configuration allows the processing of light with two polarizations at the transmitter (Tx) if electro-optical modulators can be operated with either light direction, i.e., if they are configured as lumped elements. Suitable modulators have been developed and integrated on a system chip (Section 3).

*jwitzens@iph.rwth-aachen.de; phone +49 241 80 20020; iph.rwth-aachen.de

Integrated Photonics Platforms III, edited by Roel G. Baets, Peter O'Brien, Laurent Vivien, Proc. of SPIE Vol. 13012, 130120C · © The Authors. Published under a Creative Commons Attribution CC-BY 3.0 License · doi: 10.1117/12.3026055

2. MOLDED GLASS MICRO-OPTICAL INTERPOSERS

We have adapted an isothermal glass molding process to form micro-optical interposers for coupling between a fiber array unit (FAU) and surface emitting/receiving couplers of a PIC in a compact assembly rising less than 2.7 mm above the surface of the PIC (Fig. 1) [7]. For each parallel channel, a pair of lenses images and reshapes a beam between a single mode (SM) fiber and the PIC [8]. Over 1000 lenses can be molded in parallel in a ~20 minutes thermal cycle, resulting in a high throughput per press (Fig. 1(d)). In contrast to plastic injection molding, this fabrication process has been optimized for high parallelization instead of fast sequential molding. Since molding occurs by pressing along one axis only, certain shapes, such as lenses oriented with a right angle relative to each other, are better implemented by combining two molded glass pieces together after the molding process, but other than that the molding process offers many degrees of freedom to shape glass pieces that goes well beyond the capabilities of other manufacturing techniques such as greyscale lithography. Compared to glass shaping by sequential pulsed laser exposure followed by a selective chemical etch [9], glass molding allows batch processing as well as a very high surface quality with a peak-to-trough roughness below 3 nm.

Figure 1(e) shows an interposer that has been scaled up to 32 parallel channels, with measured SM-fiber to SM-fiber insertion losses shown in Fig. 1(f). Other than for a single outlier, excess insertion losses are between 1 dB and 1.5 dB across the entire array.

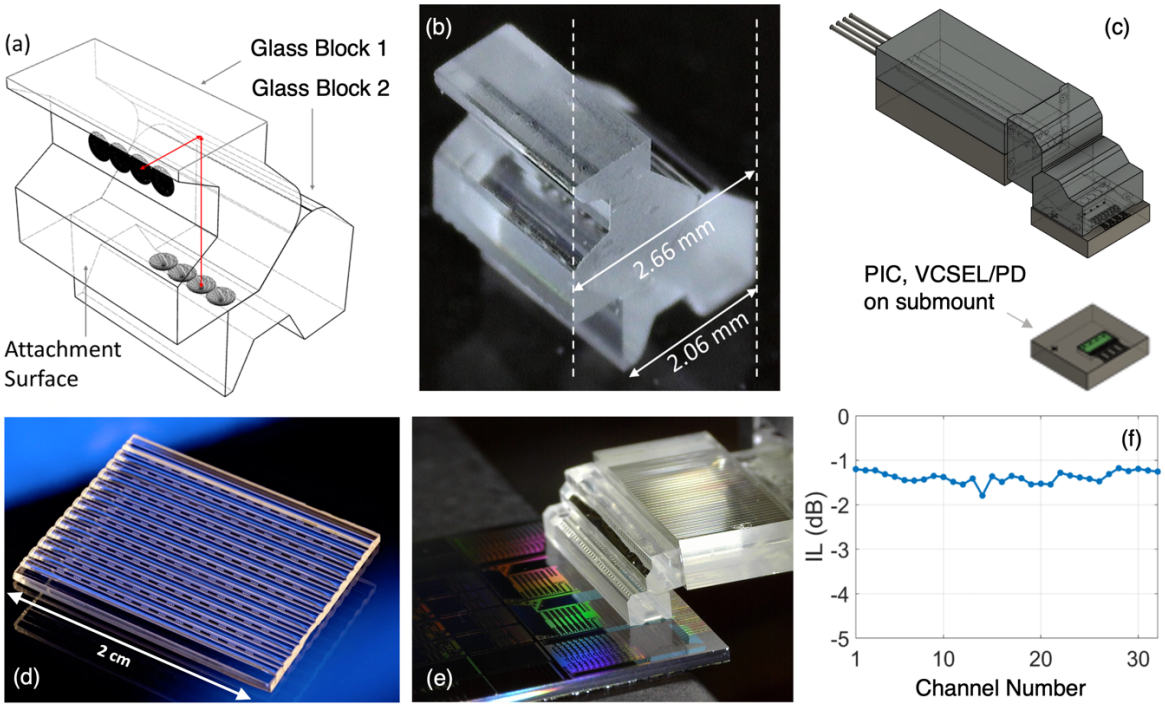

Figure 1. Glass molded micro-optical interposers for fiber coupling of PICs with surface emitting/receiving optical interfaces. (a) Schematic representation of a four-channel interposer formed by the assembly of two molded glass pieces. (b) Assembled interposer with labeled dimensions and (c) diagram of a complete assembly with FAU and PIC or submount. (d) Molded 1" glass plate with 144 groups of 4 lenses. A fully populated mold fits twice that number or arrays. (e) Interposer with 32 parallel channels and (f) measured insertion losses (SM-fiber to SM-fiber).

The internal surfaces formed where two glass pieces are merged can be used for augmenting the functionality of the devices. Figure 2 shows an example of an interposer in which a polarization splitter-combiner has been integrated. Such a device can be used to launch two polarizations into a fiber from a dual-polarization transmitter or to receive scrambled polarization from an SM-fiber [10] without incurring the excess losses and polarization dependent losses of a polarization splitting grating coupler.

Figure 2(a) shows an extrusion drawing of this interposer with beam paths shown for two different configurations, either with an FAU attached to the top or to the side of the interposer. The compact diagrams for both configurations are shown in panels (b) and (c). By intercalating Faraday rotators with a non-reciprocal 45 degree rotation between the micro-optics and single polarization grating couplers located on the PIC, isolation functionality can also be obtained.

This scheme relies on the selective deposition of a thin film coating acting as a polarization splitter on one facet of a glass building block, as schematically shown by the green area in Fig. 2(a). We did first trials for the deposition of a suitable thin-film stack by shadow masking, with results shown in Figs. 2(d) and 2(e).

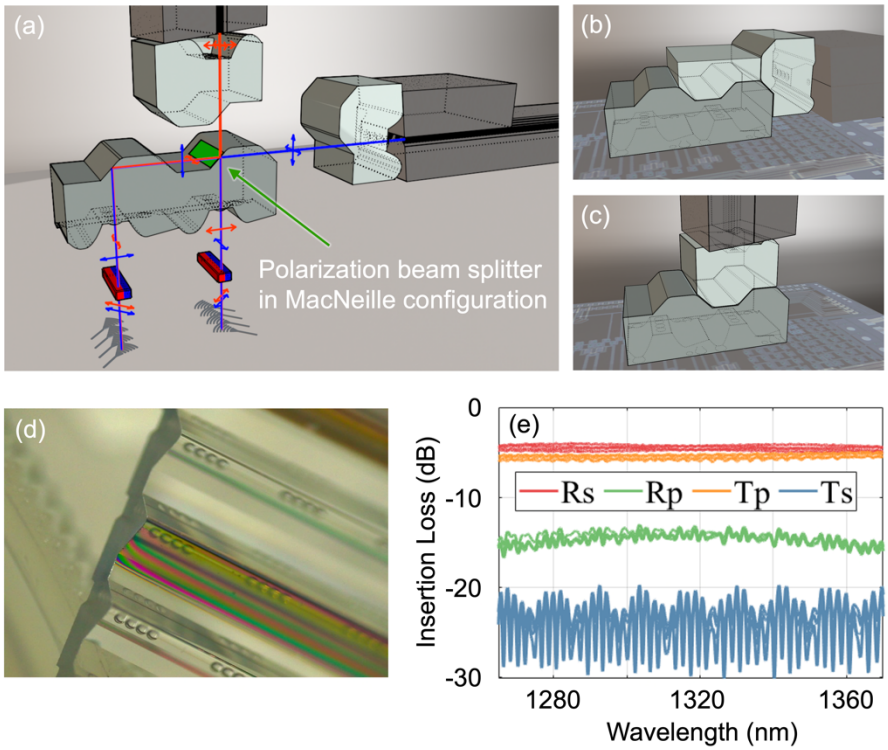

Figure 2. Glass molded micro-optical interposer with integrated polarization management. (a) Extrusion drawing of the interposer in two configurations, with an FAU attached on top or on the side of the device. The red and blue device intercalated between the single polarization grating couplers and the glass micro-optics are 45° Faraday rotators. Polarization of the light transiting through the device is represented in blue or red depending on the direction of propagation, illustrating the isolation functionality of the device. The compact representations of the two device configurations are shown in (b) and (c). (d) Glass building block after selective deposition of a thin film coating implementing a polarization splitter-combiner in MacNeille configuration, by means of shadow masking. (e) Resulting SM-fiber to SM-fiber insertion losses for the configuration shown in (c). The p-polarization is intended to be transmitted straight from the top port, represented as being coupled to an FAU, to the optical port right below (Tp), while the s-polarization is intended to be reflected at the thin-film coating and routed to the other optical port at the bottom of the device (Rs). Ts and Rp show the rejection of the unwanted polarization at the two output ports.

The thin film stack is configured to act as a polarization splitter in MacNeille configuration and was deposited by plasma enhanced chemical vapor deposition (PECVD) as alternating silicon dioxide and silicon nitride layers, with a total of 17 layers. Transfer of this process to an industrial tool better suited for optical thin film coatings is currently in progress. We are also currently working on the assembly process to reduce the insertion losses of this composite device.

With this baseline technology, more complex configurations can be devised that solve the aforementioned problem of polarization diversity in CPO transmitters. The concept relies on lumped-element electro-optic modulators by which light transiting in either direction can be modulated and is schematically shown in Fig. 3. Continuous wave (CW) light coupled from an external semiconductor laser to the package via an SM-fiber is split by polarization by the interposer and sent to two PIC ports from which it transits through the modulator in opposite directions. After modulation, each beam exits the PIC through the opposite optical port and is coupled back to the interposer. By again intercalating 45° Faraday rotators in the optical path, the assembly becomes non-reciprocal, and the returning light is sent to another optical port of the glass interposer, where it is picked up by an output fiber. As for previously demonstrated receiver (Rx) subsystems [10], the group delays have to be balanced for both polarizations, in this case between the modulator and the output fiber, by providing suitable delay loops on the PIC.

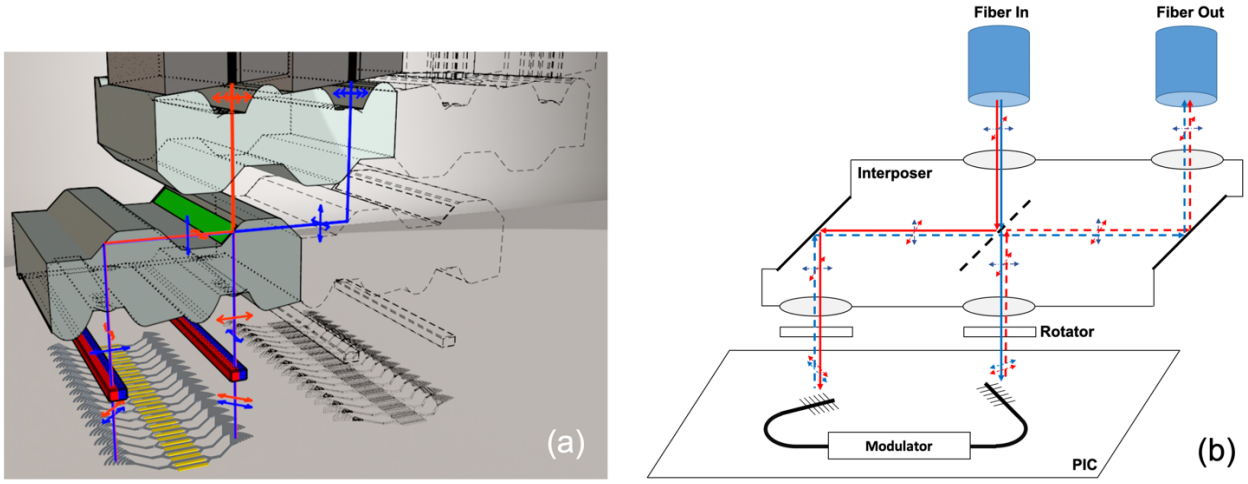

Figure 3. Interposer configuration enabling a polarization diverse CPO transmitter without requiring duplication of electro-optic modulators or on-chip polarization recombination. (a) 3D rendering and (b) schematic representation of the light path.

3. MODULATOR AND CHIP DESIGN

To support the system architecture shown in Fig. 3, we aimed at designing a suitable lumped element modulator in all-silicon technology, i.e., based on the free-carrier dispersion effect but with suitably high modulation efficiency. The device concept is based on our previous work on temperature-tolerant, resonantly assisted Mach-Zehnder modulators (MZM) [11]. To obtain a wide optical bandwidth, ring modulators acting as phase shifters are heavily over-coupled to either arm. This spoils their quality (Q-)factor and thus their linewidth, but at the same time reduces the resonant enhancement of the phase shifters. To maintain sufficient phase shift, several resonators are collectively driven on each arm. This way, the $V_\pi L\alpha$ of the phase shifters is maintained, but a resonant enhancement is obtained that can be freely traded off with the optical bandwidth of the device [12]. By shrinking the physical dimensions of the device sufficiently to make it operate as a lumped element from an electrical perspective, a very substantial additional energy consumption enhancement is obtained compared to a travelling wave device [12]. This general design concept of collectively driven low-Q resonantly enhanced phase shifters has been adapted to other resonator configurations, such as Bragg grating defects [13], [14]. In either case, great care has to be applied to not induce substantial excess optical losses due to the passive resonator design.

To increase the practicality of our initial device [11] in a datacom environment, we have ported it from the C- to the O-band and increased its optical passband, defined between the wavelengths at which the optical modulation amplitude (OMA) drops by 1 dB, to 6.6 nm [15]. This allows for example operation over a 65°C temperature range without thermal tuning of the rings, while still budgeting a fabrication tolerance of ±0.5 nm for both the laser wavelength and the fixed-temperature resonance wavelength of the rings. To achieve the 6.6 nm optical bandwidth, an additional refinement was introduced in the design:

Instead of designing all eight rings collectively driven on each arm to be nominally identical, their resonances were slightly spread so as to cover a larger wavelength range. As a consequence, at any given wavelength within the 1-dB OMA passband, an effective number of only three rings contributes to the phase modulation, reducing the resonant enhancement as a price to pay for this. Nonetheless, a resonant enhancement of 2.3 is maintained, sufficient to shrink the device to remain lumped element. Figure 4 illustrates this concept and shows a micrograph of the device and its main experimental characteristics.

The 3-dB electro-optic cutoff frequency of the fabricated modulator was measured to be 28 GHz in a 50Ω environment, in close accordance with the device models. However, the modulator was designed to be operated with a close-by lumped element driver with a low output impedance. Assuming a modulator output impedance of 7Ω, the modulator is expected to reach a 55 GHz cutoff frequency based on 3D radio-frequency (RF) simulations.

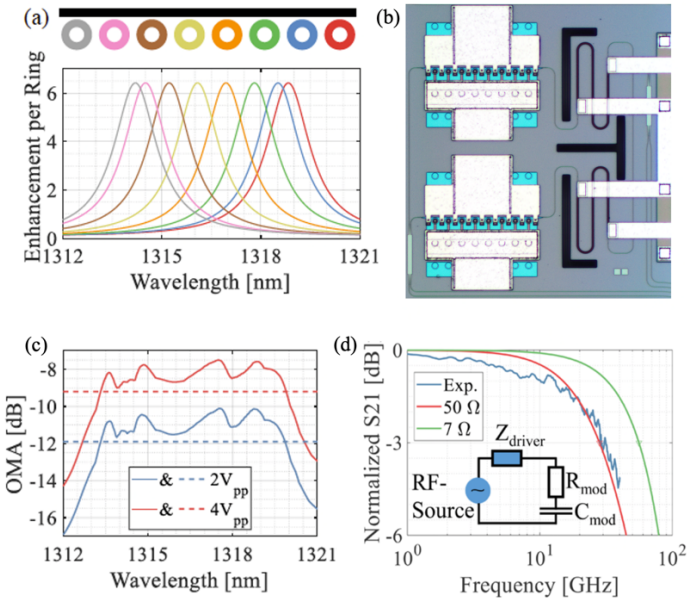

Figure 4. Resonantly assisted lumped-element modulator with a wide optical bandwidth. (a) Schematic of a single MZM arm with eight collectively driven over-coupled ring modulators with staggered resonances. (b) Micrograph of the modulator. (c) OMA as a function of wavelength for both 2 V_{pp} and 4 V_{pp} electrical differential drive. The MZM is maintained at its quadrature point with the phase shifters visible on the right of panel (b), but rings are left untuned. (d) Electro-optic S_{21} measurement in a 50Ω environment (blue curve), corresponding model (red curve) and model of the MZM driven by a lumped element driver with a 7Ω output impedance (green curve).

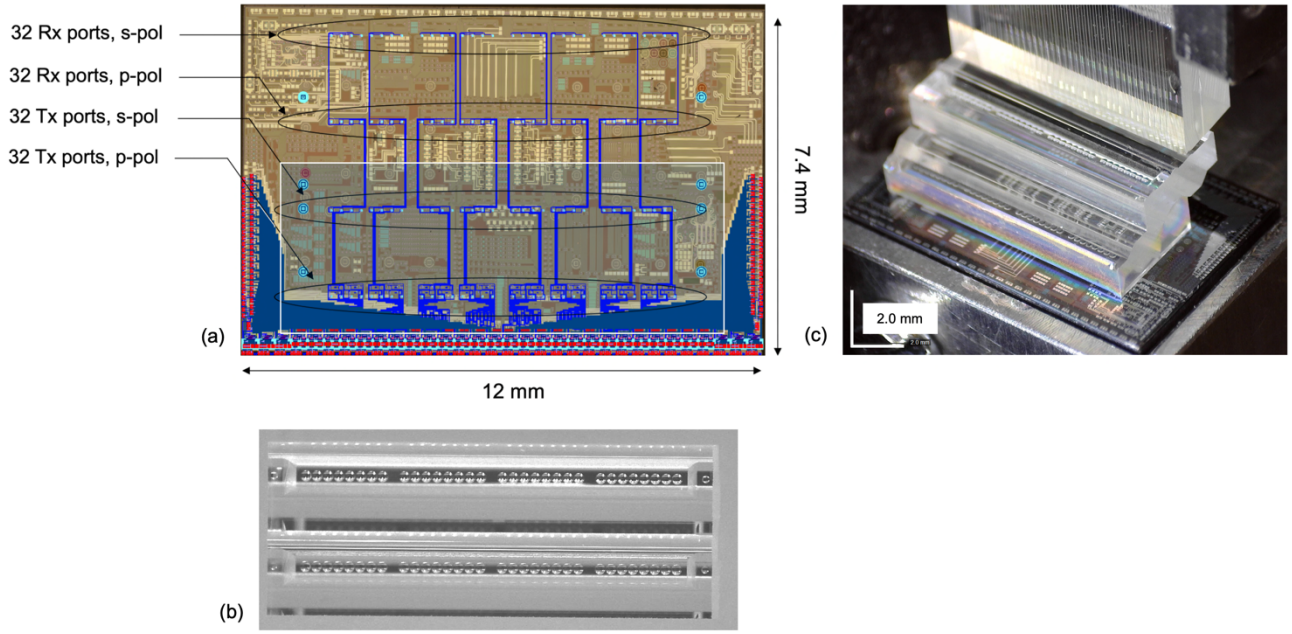

Figure 5. (a) Micrograph of the PIC overlaid with the waveguide routing of the system described in the text, in blue. (b) Micrograph of one of the two glass blocks used to build the interposer for the 32 polarization-agnostic Tx, at scale with the micrograph of the PIC. The footprint of the glass block on the PIC is shown by a white rectangle. (c) Photograph of the Tx assembly.

Figure 5(a) shows an overview of a PIC designed for the assembly scheme described in the previous section. 32 parallel transmitters and receivers are implemented on the chip. Each Tx uses the resonantly enhanced MZM described above and has two input/output ports, one for in-coupling the s-polarization and out-coupling the p-polarization and another for in-coupling the p-polarization and out-coupling the s-polarization. The Rx each have two input ports, one for in-coupling the

s-polarization and one for in-coupling the p-polarization, that are then sent to the same germanium photodiode where they are recombined [16]. Inside the chip, only the transverse electric (TE) polarization is used.

The glass interposer for the Tx-array is formed out of two molded glass pieces, one of which is represented in Fig. 5(b), at scale with the micrograph of the PIC. The complete assembly is shown in Fig. 5(c). An interposer for the entire Tx+Rx system could also be built with two glass blocks comprising four rows of lenses each.

ACKNOWLEDGEMENTS

The authors acknowledge funding from the German Federal Ministry of Education and Research for project EfficientLight, under grant 13N14964.

REFERENCES

[1] Margalit, N., Xiang, C., Bowers, S. M., Bjorlin, A., Blum, R., and Bowers, J. E., "Perspective on the future of silicon photonics and electronics," Appl. Phys. Lett. 118, 220501 (2021).
[2] Maniotis, P., Schares, L., Kuchta, D. M., and Karacali, B., "Towards higher-radix switches with co-packaged optics for improved network locality in data center and HPC networks," Opt. Comm. & Network. 14(6), C1–C10 (2022).
[3] Hosseini, K. *et al.*, "8 Tbps Co-Packaged FPGA and Silicon Photonics Optical IO," in Proc. Opt. Fib. Comm. Conf. (OFC), Th4A.2 (2021).
[4] Trott, G. R. and Shorey, A., "Glass Wafer Mechanical Properties: A Comparison To Silicon," in Proc. Int. Microsys., Packaging, Assembly & Circ. Technol. Conf., 359–362 (2011).
[5] Mekis, A., Narasimha, A., and Witzens, J., "Method and system for integrated power combiners," US Patent US8625935B2, filed Jun. 2011.
[6] Lin, Z. *et al.*, "High-performance polarization management devices based on thin-film lithium niobate," Light: Sci. & Appl. 11, 93 (2022).
[7] Merget, F., Ackermann, M., Shen, B., Saunders, G. D., Haag, S., Wolz, M., and Witzens, J., "Glass Molded Optical Interposers for Wafer Scale Datacom Component Packaging," in Proc. 2021 Europ. Conf. on Opt. Comm. (ECOC).
[8] Ackermann, M., Shen, B., Merget, F., Wolz, M., and Witzens, J., "Glass-molded optical interposers for wafer scale photonic integrated circuit packaging in 800G modules and co-packaged optics," in Proc. SPIE 12007, 120070M (2022).
[9] Marcinkevicius, A. *et al.*, "Femtosecond laser-assisted three-dimensional microfabrication in silica," Opt. Lett. 26(5), 277–279 (2001).
[10] Nojic, J., Schoofs, D., Sharif Azadeh, S., Merget, F., and Witzens, J., "Polarization-diverse silicon photonics WDM receiver with a reduced number of OADMs and balanced group delays," in Proc. Opt. Fib. Comm. Conf. (OFC), M4H.2 (2020).
[11] Romero Garcia, S., Moscoso-Martir, A., Sharif Azadeh, S., Müller, J., Shen, B., Merget, F., and Witzens, J., "High-speed resonantly enhanced silicon photonics modulator with a large operating temperature range," Opt. Lett. 42(1), 81–84 (2017).
[12] Witzens, J., "High-speed silicon photonics modulators," Proceedings of the IEEE 106(12), 2158–2182 (2018).
[13] Jafari, O., Shi, W., Larochelle, S., "Mach-Zehnder Silicon Photonic Modulator Assisted by Phase-Shifted Bragg Gratings," IEEE Photon. Technol. Lett. 32(8), 445–448 (2020).
[14] Han, C. *et al.*, "Slow-light silicon modulator with 110-GHz bandwidth," Sci. Adv. 9, eadi5339 (2023).
[15] Ackermann, M., Moscoso-Martir, A., Shen, B., Merget, F., and Witzens, J., "Resonantly enhanced lumped-element O-band Mach-Zehnder modulator with an ultra-wide operating wavelength range," Opt. Lett. 48(21), 5623–5626 (2023).
[16] Kucharski, D., Guckenberger, D., Masini, G., Abdalla, S., Witzens, J., and Sahni, S., "10Gb/s 15mW optical receiver with integrated Germanium photodetector and hybrid inductor peaking in 0.13 μm SOI CMOS technology," in Proc. IEEE Int. Sol.-Stat. Circ. Conf. (ISSCC), 360–361 (2010).